

## RAMAN MICROPROBE SPECTROSCOPY OF HALLOYSITE

R.L. FROST AND H.F. SHURVELL†

Centre for Instrumental and Developmental Chemistry, Queensland University of Technology, Brisbane, Q 4001, Australia

**Abstract**—The Raman spectra of a tubular halloysite originating from Matauri Bay, New Zealand, have been obtained using a Renishaw 1000 Raman microscope system. The Raman microprobe enables the Raman spectra of crystals as small as 0.8  $\mu\text{m}$  diameter to be obtained over the complete wavelength range and allows spectral variations along the different crystal axes to be studied. Three bands in the hydroxyl stretching region were observed at 3616.5, 3623.4 and 3629.7  $\text{cm}^{-1}$  and are attributed to the inner hydroxyls of the shared lower plane of the octahedral sheet of the halloysite. Two bands at 3698.2 and 3705  $\text{cm}^{-1}$  were obtained for the outer hydroxyls of the unshared outer octahedral plane. The relative intensity of the 3629.7  $\text{cm}^{-1}$  band varied according to the tube orientation. Lattice vibrations of the halloysite were also found to be orientation-dependent.

**Key Words**—Halloysite, Kaolinite, Lattice Vibrations, Raman Microprobe, Raman Spectroscopy.

### INTRODUCTION

Raman spectroscopy has been used to a limited extent in the study of the kaolinite clay minerals (Johnston et al 1985; Michaelian 1986; Wiewióra et al. 1979). Fourier transform Raman spectroscopy has been shown to be very useful for the structural elucidation of the kaolinite clay mineral structure (Frost et al. 1994; Frost 1995). However, the only published Raman microprobe spectroscopy (RMS) of kaolinite is a study of the temperature dependence of the hydroxyl stretching region of kaolinite (Pajcini and Dhamelin-court 1994). To date, no RMS work has been published on halloysite.

The halloysite structure consists of kaolinite-like aluminosilicate layers interspersed in the fully hydrated mineral with a sheet of water molecules (Newman 1987). Halloysite, as with the other polymorphs of kaolinite, contains 2 types of hydroxyl groups: 1) the outer hydroxyl groups (OuOH) and 2) the inner hydroxyl groups (InOH). The OuOH are situated in the outer-upper unshared plane, whereas the InOH groups are located in the lower shared plane of the octahedra sheet. The usual morphology of halloysite is tubular, with 1 or more layers rolled spirally (Dixon and McKee 1974). In the fully hydrated state, the inter-layer spacing of halloysite is 10.1 Å. Upon dehydration, the spacing decreases to 7.2 Å. The halloysite samples used in this Raman study are all dehydrated samples.

### EXPERIMENTAL

Halloysite clay mineral samples were placed on a polished metal surface on the stage of an Olympus BH2-UMA microscope, which is equipped with 10 $\times$ , 20 $\times$ , and 50 $\times$  objectives. No sample preparation was

needed, apart from some flattening of the clay sample. The microscope is part of a Renishaw 1000 Raman microscope system, which also includes a monochromator, a filter system and a charge-coupled detector (CCD). Raman spectra in the hydroxyl stretching region were excited by a Spectra-Physics Model 127 He/Ne laser operating at 633 nm. Spectra in the lattice mode region (150–1200  $\text{cm}^{-1}$ ) were excited by the 780-nm line of a diode laser. The spectra were recorded at a resolution of approximately 2  $\text{cm}^{-1}$  and were acquired in sections of approximately 800  $\text{cm}^{-1}$ , or as extended scans. The area of laser excitation of the halloysite is  $\sim 0.64 \mu\text{m}^2$  when the 50 $\times$  objective is being used. Repeated acquisitions were accumulated to improve the signal-to-noise ratio in the spectra. Normally, eight 60-s scans at  $\times 50$  provide reasonable quality spectra for both the hydroxyl stretching and lattice regions. Spectral calibration was carried out using the 520.5- $\text{cm}^{-1}$  line of a silicon wafer, and wavenumbers reported in the tables are correct to  $\pm 1 \text{ cm}^{-1}$ .

Spectral manipulation such as baseline adjustment, smoothing and normalization were performed using the Spectrocalc software package GRAMS<sup>®</sup> (Galactic Industries Corporation, New Hampshire). Band component analysis was carried out using the peakfit software package by Jandel Scientific. Lorentz-Gauss cross-product functions were used throughout and peak fitting carried out until correlation coefficients of  $>0.997$  were obtained.

### RESULTS AND DISCUSSION

The Raman spectra of the hydroxyl stretching region of halloysite are shown in Figure 1. The spectra are much weaker than those of the other kaolinite clay minerals and only 2 clear maxima are observed near 3705 and 3630  $\text{cm}^{-1}$ . Shoulders are observed at 3635 and 3620  $\text{cm}^{-1}$  on the low-frequency band. The intensity of the strong shoulder at 3635  $\text{cm}^{-1}$  varies when

† Permanent address: Department of Chemistry, Queen's University, Kingston, Ontario, Canada K7L 3N6.

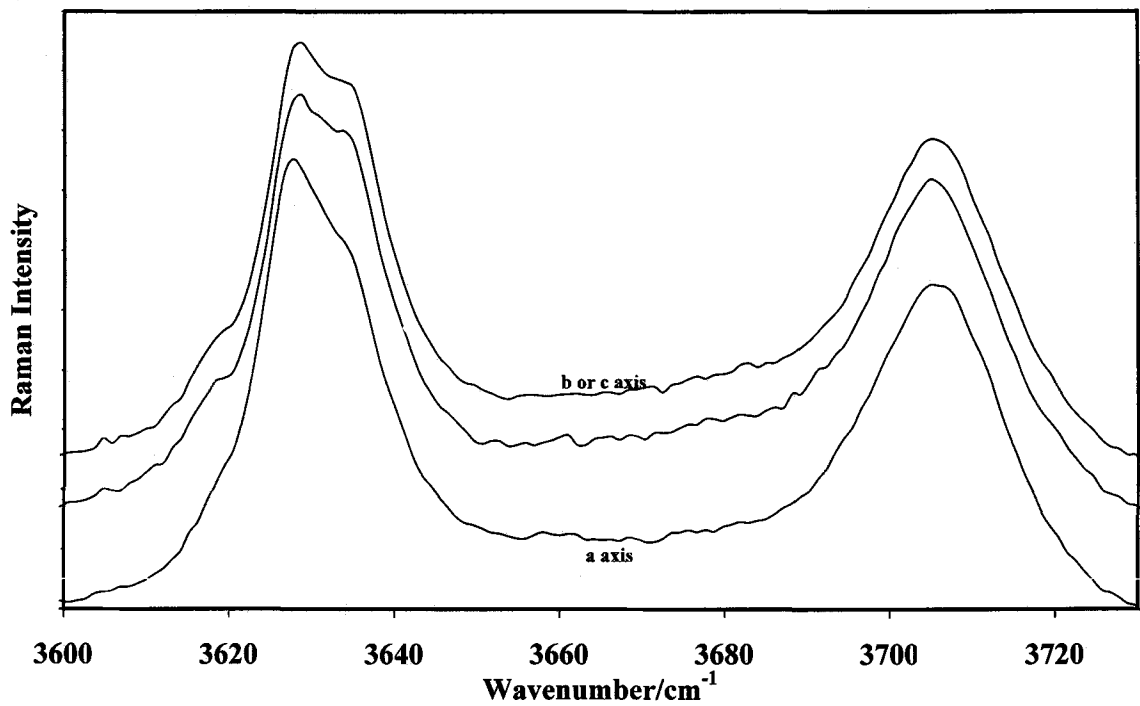


Figure 1. Raman spectrum of the hydroxyl stretching region of halloysite irradiated along the *a*, *b* and *c* axes.

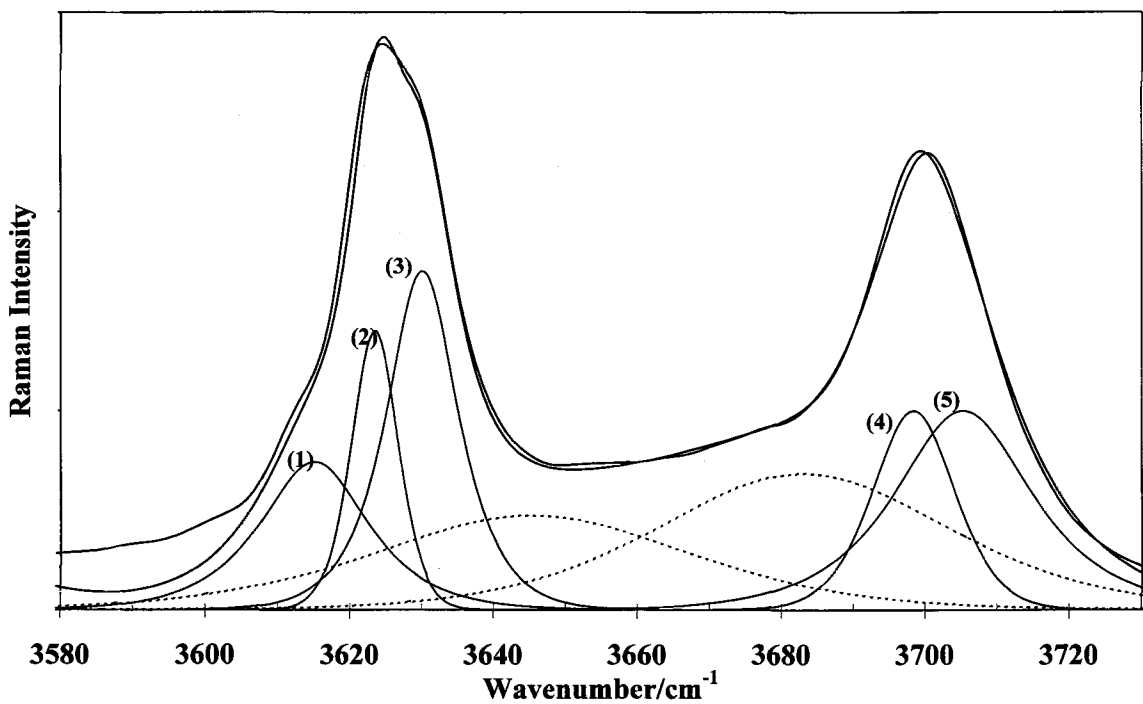


Figure 2. The band component analysis of the hydroxyl stretching region of halloysite.

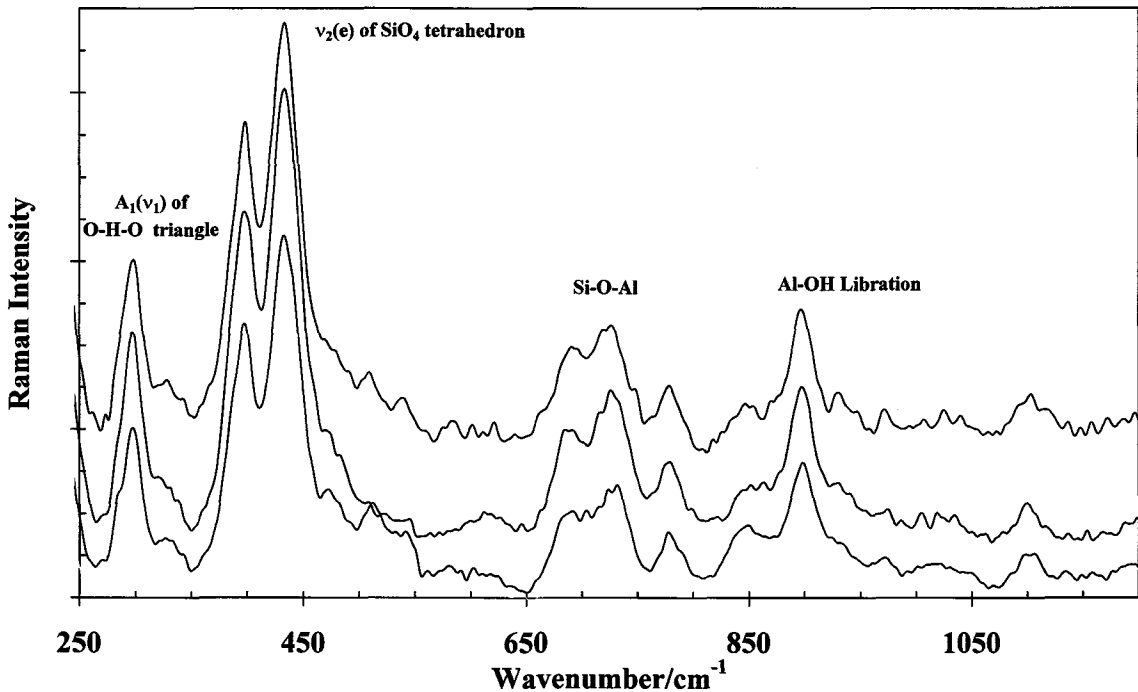


Figure 3. The Raman spectrum of the lattice regions of halloysite.

the spectrum is recorded from crystals with different orientations. Halloysite differs from the other clay minerals by the presence of water molecules in the structure, and the tubular morphology of halloysite crystals implies that there are only 2 different excitation directions. These are along the tube axis, the *a* axis and, in the direction perpendicular to it, the *c* or *b* axis. It is suggested that the spectra of Figure 1 correspond to excitation approximately in these 2 directions. The top 2 spectra were determined for the alignment of the laser at right angles to the tubes: i.e., along the *b* and *c* axes of the crystals. The 3rd spectrum is obtained when the laser is directed along the tubes: i.e., along the *a* axis of the halloysite crystals. Variation in intensity of the hydroxyl region band profile between 3600 and 3650  $\text{cm}^{-1}$  is observed.

Band component analysis of the hydroxyl stretching region was undertaken. A Lorentz-Gauss cross-prod-

Table 1. The results of the band component analysis of the hydroxyl stretching region of the Raman spectrum of halloysite from Figure 2.

	Band 1 ( $\text{cm}^{-1}$ )	Band 2	Band 3	Band 4	Band 5
Spectrum <i>b</i> or <i>c</i> axis	3616.5	3623.4	3629.7	3698.2	3705.2
	8.3	4.8	6.3	7.2	11.1
	10%	7.5%	14.3%	9%	16%
Spectrum <i>a</i> axis	3616.4	3623.4	3629.8	3698.2	3705.0
	8.4	4.7	6.3	7.3	11.2
	11%	9%	10%	9.2%	16.2%

uct function was used and a Lorentz/Gauss ratio of 0.7 was used for all bands. Seven component bands were required to fit the observed band envelope. The results of this analysis are shown in Figure 2, and the parameters of the resolved components are reported in Table 1. The table shows the band centers and half-widths (as half-widths at half-height) and the percentage area of each component band. Three components of the in-

Table 2. The band positions and suggested assignments of the observed bands in the lattice region of halloysite.

Band center ( $\text{cm}^{-1}$ )	Suggested assignments
134.7	O-Si-O bend of the $\text{Si}_2\text{O}_5$ unit
156	O-Al-O symmetric bend of inner surface hydroxyl
168	
172	O-Al-O symmetric bend of inner hydroxyls
179	
192	O-H-O symmetric bend
208	
238	O-H-O symmetric stretch
298	O-H-O antisymmetric stretch
396	Si-O deformation
442	Al-O stretch
510	Si-O bend
540	Si-O bend
693	$\nu_1(a_1)$ mode of $\text{SiO}_4$
728	OH translation
779	OH translation
844	Si-O-Al deformation
910	Al-OH libration
1100	SiO stretch

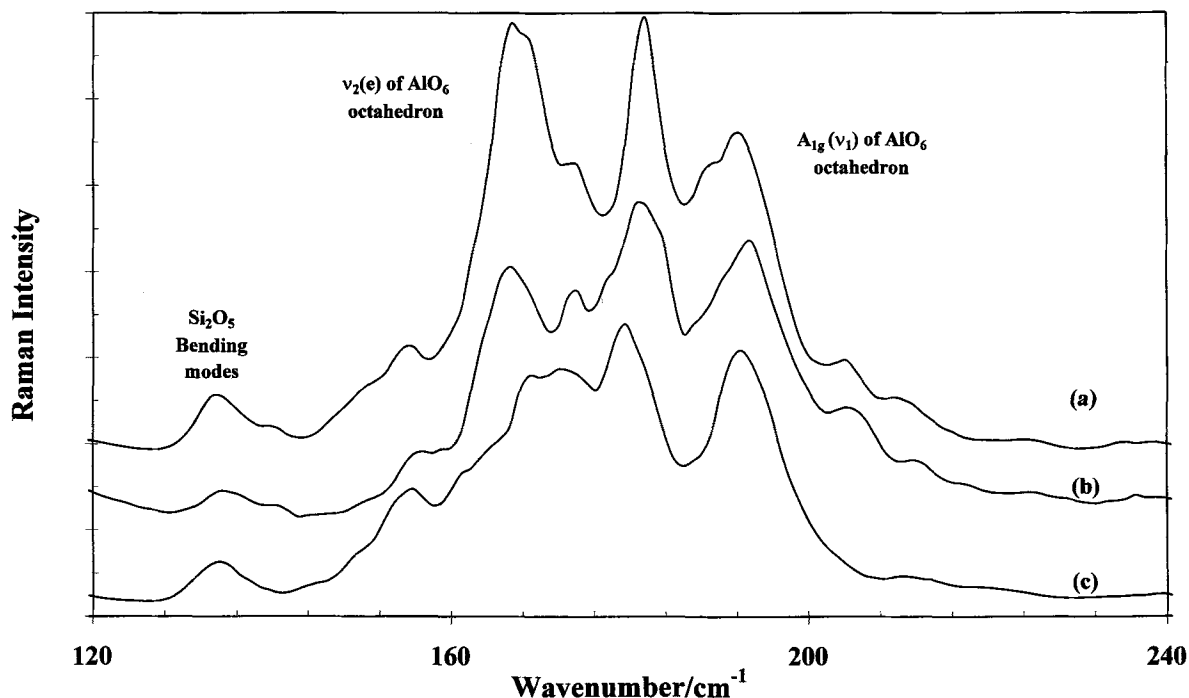


Figure 4. The Raman spectrum of the lattice regions of halloysite in the 120 to 250  $\text{cm}^{-1}$  region showing orientation dependence of the spectra.

ner hydroxyl groups are identified at 3616.5, 3623.4 and 3629.7  $\text{cm}^{-1}$ . The bands are sharp, with half-widths of 8.3, 4.8 and 6.3  $\text{cm}^{-1}$ , respectively. These sharp bands are indicative of 3 different environments of the inner hydroxyl groups controlled by hydrogen bonding and the dioctahedral spaces in the adjacent silica layer into which these hydroxyl groups point. The folding of the halloysite layers has resulted in the formation of 3 different hydroxyl groups in this region. In kaolinite, only a single symmetric band is found in the Raman microprobe spectrum (Pajcini 1994). The outer hydroxyl that points away from the aluminum layer gives rise to 2 overlapping bands centered at 3698 and 3705  $\text{cm}^{-1}$  with half-widths of 7.2 and 11.2  $\text{cm}^{-1}$ . It is hypothesised that these 2 bands arise from positional disorder brought about by the folding of the octahedral sheets. The bands at 3645 and 3682  $\text{cm}^{-1}$  have been best described as the out-of-phase vibrations of the in-phase vibrations at 3698 and 3705  $\text{cm}^{-1}$  (Brindley et al. 1986). Similar bands are observed in kaolinites at 3650 and 3670  $\text{cm}^{-1}$  (Frost 1995).

Figure 3 shows the Raman spectrum of the lattice region of the halloysite. Table 2 reports the spectral positions of these bands. The observed spectra in the lattice mode region of halloysite can be interpreted in terms of the vibrations of the repeating unit in the structure of the mineral ( $\text{Al}_2(\text{OH})_4\text{Si}_2\text{O}_5$ ), in the present case. It has been suggested (Loh 1973) that these vibrations can be treated as those of distorted  $\text{AlO}_6$  oc-

tahedra of symmetry  $S_6$ , distorted  $\text{SiO}_4$  tetrahedra of symmetry  $C_{3v}$ , an O-H-O group of symmetry  $C_{2v}$  and bending modes of the OH groups. Other workers have simply classified the vibrations as lattice modes. The suggested assignments of the observed features given in Table 2 are based on previously published work on layer silicates (Farmer 1974; Farmer and Russell 1964; Ishii et al. 1967).

Figure 4 illustrates the variation in intensity of the bands in the 120 to 240  $\text{cm}^{-1}$  region for a selection of different halloysite crystals. A considerable number of spectra in this region were obtained, but the spectra reduce to a combination of 2 or more of the illustrated spectra. The band at 134.7  $\text{cm}^{-1}$  is attributed to the symmetric bending mode of the  $\text{Si}_2\text{O}_5$  unit of halloysite (Ishii et al. 1967). Some variation in the peak position is observed for this band and 2 bands are observed in the spectra of A and B. The bands at 156, 168, 172 and 179  $\text{cm}^{-1}$  are attributed to the O-Al-O symmetric bends of the  $\text{AlO}_6$  octahedra. These bands correspond to the symmetric stretching vibrations of the Al-OH groups shown in Figure 2. One possibility is that the band at 156  $\text{cm}^{-1}$  is associated with the hydroxyl stretching vibration of the outer hydroxyl. The 3 other bands of the O-Al-O symmetric bends of the  $\text{AlO}_6$  octahedra are associated with the 3 inner hydroxyls. The intensities of these bands help to confirm their assignment as symmetric vibrations.

The 2 bands at 192 and 208  $\text{cm}^{-1}$  are due to the symmetric O-H-O bends in halloysite. Loh assigned

bands in the 200 to 300  $\text{cm}^{-1}$  region of the Raman spectra of sheet silicates to vibrations of the triangular O-H-O group. In the present spectra, bands observed near 238 and 298  $\text{cm}^{-1}$  could be attributed to these vibrations. All of these 3 bands are found to be orientation-dependent, and it is considered that the bands are composed of 2 or more component bands. Farmer and Russell (1964) attributed a group of infrared bands between 400 and 540  $\text{cm}^{-1}$  to Si-O-Al stretching and Al-OH bending modes. The 2 bands at 396 and 442  $\text{cm}^{-1}$  for halloysite are attributed to these 2 vibrations. These authors also assign infrared bands near 935 and 914  $\text{cm}^{-1}$  in kaolinite clay minerals to OH bending vibrations and a band near 757  $\text{cm}^{-1}$  to vibrations of the octahedral  $\text{Al}^{3+}$  ions and the hydroxyl groups on the side of the tetrahedral layer. In halloysite, it is found that there is a single band at 910  $\text{cm}^{-1}$  and that the band at 757  $\text{cm}^{-1}$  is split into 2 components at 728 and 779  $\text{cm}^{-1}$ .

### CONCLUSIONS

This research shows the potential application of RMS to research into clay minerals. The spectra are shown to be orientation-dependent. New insights into the structure of halloysites can be obtained using RMS. The technique offers a simple and rapid method for identification and characterization of clay minerals. Furthermore, the technique allows the possibility of studying clay-organic interactions, since the Raman bands of soil organics will be in a different part of the spectral region.

The technique has several major advantages: 1) spectra from the individual faces of the crystal can be measured; 2) minerals containing very small amounts of the particular mineral can be analyzed; and 3) it is particularly useful for the analysis of the hydroxyl stretching region of minerals. Where fluorescence is not a problem or can be minimized, the technique is extremely useful for the study of the lattice region of minerals. The use of the diode laser operating at 780 nm eliminates most of the fluorescence that is normally associated with the Raman spectroscopy of min-

erals. The possibility of obtaining spectra from very small crystals with different orientations opens up possibilities for future structural and morphological studies.

### ACKNOWLEDGMENTS

Dr S. Van der Gaast of the Netherlands Institute for Sea Research is thanked for many helpful discussions. Support for this research by the Queensland University of Technology Centre for Instrumental and Developmental Chemistry is also gratefully acknowledged.

### REFERENCES

- Brindley GW, Chih-Chun Kao, Harrison JL, Lipsicas M, Raythatha R. 1986. Relation between the structural disorder and other characteristics of kaolinites and dickites. *Clays Clay Miner* 34:233-249.
- Dixon JB, McKee TR. 1974. Internal and external morphology of tubular and spheroidal halloysite particles. *Clays Clay Miner* 22:127-137.
- Farmer VC, Russell JP. 1964. Infrared spectra of silicates. *Spectrochim Acta* 20:1149-1173.
- Farmer VC, editor. 1974. Infrared spectra of minerals, Ch 15. London: Mineral Soc. p 331-363.
- Frost RL. 1995. Fourier transform Raman spectroscopy of kaolinite, dickite and halloysite. *Clays Clay Miner* 43:191-195.
- Frost RL, Fredericks PM, Bartlett JR. 1994. Fourier transform Raman spectroscopy of kandite clays. *Spectrochim Acta* 20:667-674.
- Ishii M, Shimanouchi T, Nahahira M. 1967. Far infrared absorption spectra of micas. *Inorg Chim Acta* 1:387.
- Johnston CT, Sposito G, Birge RR. 1985. Raman spectroscopic study of kaolinite in aqueous suspension. *Clays Clay Miner* 33:483-489.
- Loh E. 1973. Optical vibrations in sheet silicates. *J Phys C: Solid State Phys* 6:1091-1104.
- Michaelian KH. 1986. The Raman spectrum of kaolinite #9 at 21 °C. *Can J Chem* 64:285-289.
- Newman ACD, editor. 1987. Chemistry of clays and clay minerals, Ch 5. Mineral Soc monograph 6. London: Longman. p. 237-274.
- Pajcini V, Dhamelincourt P. 1994. Raman study of the OH-stretching vibrations in kaolinite at low temperature. *Appl Spectrosc* 48:638-641.
- Wiewióra A, Wieckowski T, Sokolowska A. 1979. The Raman spectrum of the kaolinite sub-group. *Arch Mineral* 135:5-12.
- (Received 9 February 1996; accepted 11 April 1996; Ms. 2736)